Cartilage Injury
Update on Diagnosis and Image-guided Therapy

Josue Solís-Ugalde, MD[a], Teodoro Martín-Noguerol, MD[b], M. Luisa Nieto-Morales, MD, PhD[c], Carolina Díaz-Angulo, MD[d], Joan C. Vilanova, MD, PhD[e,*]

KEYWORDS

• Cartilage injury • MR imaging • Compositional MR imaging • Image-guided therapy

KEY POINTS

- MR imaging provides the reference standard for a comprehensive structural and biochemical evaluation of cartilage integrity.
- Functional MR imaging enables early detection of collagen disorganization and proteoglycan loss before morphologic defects appear.
- Standardized classifications support decision-making: Outerbridge, International Cartilage Repair Society, and Noyes–Stabler systems improve MR imaging–arthroscopy correlation and guide treatment strategy.
- Image-guided therapy improves precision: Ultrasound is first-line, while MR imaging or MR imaging–US fusion enhances accuracy in regenerative intra-articular procedures.
- Postrepair monitoring using the standardized MOCART 2.0 scoring system evaluates graft maturation, integration, and long-term outcomes.

INTRODUCTION

Cartilage injury represents a major cause of musculoskeletal pain and disability worldwide. Articular cartilage is an avascular, aneural, and alymphatic tissue, which limits its capacity for spontaneous repair once damaged. If untreated, cartilage defects often progress to osteoarthritis, leading to irreversible joint degeneration and substantial socioeconomic impact.[1] MR imaging has become the reference standard for noninvasive cartilage evaluation.[2] It allows detection of both structural damage and early biochemical alterations, providing valuable information for treatment selection, monitoring repair, and predicting outcomes. MR imaging-based biomarkers are now recognized as essential tools for the assessment of cartilage integrity and the effectiveness of regenerative and pharmacologic interventions.[3]

CARTILAGE ANATOMY

Nature creates complex systems—like forests and joints—that function optimally despite apparent disorder (**Fig. 1**). The human osteochondral unit is one such design, composed of hyaline cartilage, subchondral bone, and subarticular spongiosa, working together to absorb pressure, distribute loads, and reduce joint friction. Articular cartilage

[a] Department of Radiology, Traumatology Hospital, San José 40104, Costa Rica; [b] MRI Unit, Department of Radiology, HT Medica, Jaén, Spain; [c] Department of Radiology, Hospital Universitario Nuestra Señora de la Candelaria, Santa Cruz de Tenerife, Spain; [d] Department of Radiology, Hospital Covadonga, HT Medica, Spain; [e] Department of Radiology, Clínica Girona, Institute of Diagnostic Imaging (IDI) Girona, School of Medicine, University of Girona, Spain

* Corresponding author. Department of Radiology, Clínica Girona, Carrer Barcelona 206, 17005 Girona, Spain.
E-mail address: kai.vilanova@gmail.com

Magn Reson Imaging Clin N Am ■ (2026) ■–■
https://doi.org/10.1016/j.mric.2026.05.002
1064-9689/26/© 2026 Elsevier Inc. All rights are reserved, including those for text and data mining, AI training, and similar technologies.

Abbreviations

2D	2 dimensional
3D	3 dimensional
ACI	autologous chondrocyte implantation
ACI/MACI	autologous chondrocyte implantation
ADC	apparent diffusion coefficient
AI	artificial intelligence
BMAC	bone marrow aspirate concentrate
dGEMRIC	delayed gadolinium-enhanced MR imaging of cartilage
DWI/DTI	diffusion-weighted and diffusion tensor imaging
FSE	fast spin echo
GAG	Glycosaminoglycan
gagCEST	GAG chemical exchange saturation transfer
HA	hyaluronic acid
ICRS	International Cartilage Repair Society
MFX	Microfracture
MOCART	Magnetic Resonance Observation of Cartilage Repair Tissue
MSCs	mesenchymal stem cells
OAT	osteochondral autograft transfer
OCA	osteochondral allograft transplantation
OCL	osteochondral lesion
PD	proton-density
PGs	Proteoglycans
PRP	platelet-rich plasma
SNR	signal-to-noise ratio
SPGR	spoiled gradient recalled echo

forms part of the osteochondral unit, a biomechanically integrated complex that includes hyaline cartilage, the subchondral bone plate, and the underlying spongiosa.[4] Hyaline cartilage consists primarily of water, type II collagen, and proteoglycans. It is organized into 3 distinct zones: the superficial zone, composed of densely packed collagen fibers aligned parallel to the surface and providing resistance to shear stress; the middle zone, containing randomly oriented collagen fibers and abundant proteoglycans that contribute to elasticity; and the deep zone, characterized by perpendicular collagen bundles anchored to the calcified cartilage and subchondral bone, which provide compressive strength (see **Fig. 1**).[4] The interface between calcified cartilage and bone—the so-called tidemark—acts as a "cement line," maintaining mechanical continuity without allowing vascular or cellular intermixing. Subchondral bone ensures metabolic exchange through microvascular channels that connect to the spongiosa, maintaining the homeostasis of the overlying avascular cartilage.

MR IMAGING TECHNIQUES FOR CARTILAGE ASSESSMENT

MR imaging provides visualization of the cartilage surface and internal architecture (**Fig. 2**).[5] Continuous advances in coil design, gradient performance, and parallel imaging have increased spatial resolution and signal-to-noise ratio (SNR),[6] while artificial intelligence (AI)-based reconstruction now enables faster denoising and improved contrast-to-noise efficiency.[7]

Morphologic MR Imaging Sequences

Morphologic MR imaging sequences remain the cornerstone for routine cartilage evaluation (**Table 1**). High-resolution 2 dimensional (2D) and 3 dimensional (3D) sequences, such as proton-density (PD) fat-suppressed, T2-weighted fast spin echo (FSE), and 3D spoiled gradient recalled echo (SPGR) or (Sampling Perfection with Application-optimized Contrasts using different flip-angle Evolutions [SPACE]) techniques, provide excellent contrast between cartilage, subchondral bone, and joint fluid (**Fig. 3**).[6] These sequences permit accurate evaluation of cartilage thickness, surface regularity, and intrinsic signal changes associated with early degeneration.[8] Among the most relevant innovations, ultrashort echo time and zero echo time imaging techniques extend MR imaging sensitivity to short-T2 tissues such as calcified cartilage, improving visualization of deep layers and mineralization patterns previously invisible in standard sequences.[9]

Functional MR Imaging Sequences

Beyond morphology, functional MR imaging techniques have expanded diagnostic capability by revealing the biochemical status of the cartilage matrix before structural breakdown occurs (**Table 2**). These methods measure the interaction of water, collagen, and proteoglycans (PGs), key determinants of cartilage health. T2 mapping quantifies collagen orientation and hydration; increased T2 relaxation times indicate collagen disorganization and increased water content (**Fig. 4**).[10] Clinical application of cartilage compositional imaging is limited by high variability and suboptimal reproducibility of the biomarkers. The Quantitative Imaging Biomarkers Alliance has provided some recommendations for clinical researchers, clinicians, and industry scientists pertaining to image data acquisition, analysis, and interpretation and assessment procedures for T1ρ and T2 cartilage imaging and test–retest conformance.[3] T1rho mapping measures spin–lattice relaxation in the rotating frame and reflects PG content, making it

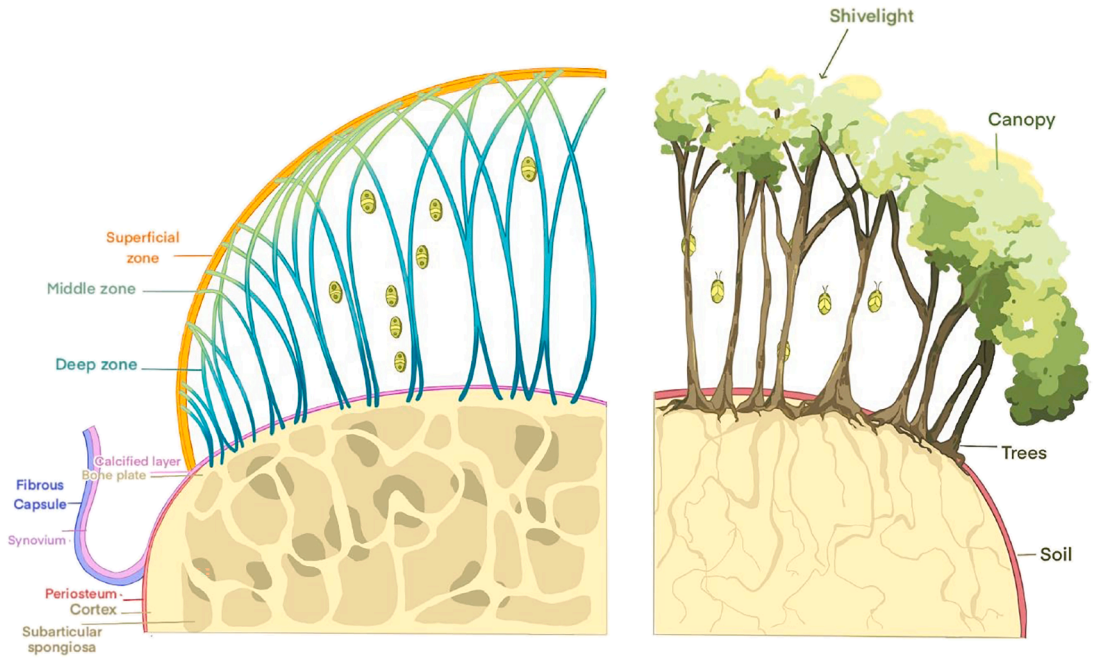

Fig. 1. Comparison between articular cartilage structure and a forest ecosystem. Collagen fibers and chondrocytes in the cartilage zones (superficial, middle, and deep) are paralleled by trees and canopy layers, highlighting the layered organization and functional depth of cartilage tissue.

particularly sensitive to early proteoglycan depletion.[11] Delayed gadolinium-enhanced MR imaging of cartilage (dGEMRIC) indirectly assesses glycosaminoglycan (GAG) concentration using negatively charged gadolinium-diethylenetriamine pentaacetic acid ($Gd\text{-}DTPA^{2-}$) contrast; low gadolinium-enhanced T1-weighted imaging (T1Gd) values correspond to reduced GAG and early degeneration.[12] Diffusion-weighted and diffusion tensor imaging (DWI/DTI) evaluate water motion within the extracellular matrix, with increased apparent diffusion coefficient (ADC) values indicating matrix disruption and collagen loss (**Fig. 5**).[13] GAG chemical exchange saturation transfer (gagCEST) MR imaging quantifies GAG concentration through proton exchange without contrast, while sodium MR imaging measures fixed charge density from sodium ion concentration, providing a noninvasive estimate of GAG content.[14]

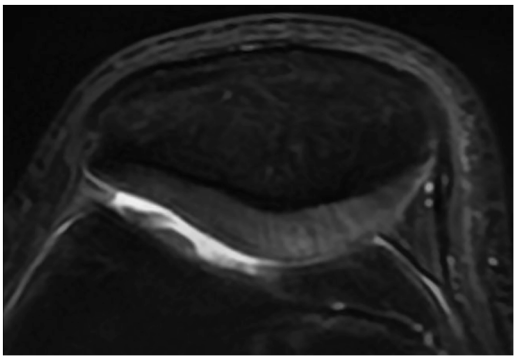

Fig. 2. A 25 year old male patient with no anterior patella pain. Axial proton density—fat saturated images show a normal, homogenous signal cartilage, with smooth surface. Grade 0. Outerbridge and ICRS.

CARTILAGE INJURY CLASSIFICATION

Standardized classification systems for cartilage injury are essential for communication,[15] treatment planning, and comparison of clinical outcomes.[16] The existence of different classification systems highlights the need for developing a standardized and clinically meaningful classification system, among other challenges that need to be faced in the near future. Arthroscopy remains the gold standard for grading, but MR imaging adaptations allow reliable noninvasive correlation with surgical findings. It is relevant in order to be concise in the radiology report to have clarity of the different terms used to describe each of the MR imaging findings (**Fig. 6**, **Table 3**). The most widely used systems include Outerbridge, International Cartilage Repair Society (ICRS), and Noyes–Stabler classifications. Lesions are typically categorized into 4 major categories, as edema only, superficial partial-thickness defects affecting less than 50% of the cartilage, deep partial-thickness

Table 1
Summary of morphologic MR imaging sequences for cartilage assessment

Sequence Type	Main Features	Advantages	Limitations	Typical Applications
2D PD or T2-weighted with fat suppression	2D FSE with intermediate weighting and fat suppression	• Excellent contrast between cartilage and joint fluid • Clear visualization of cartilage and soft tissues • Short acquisition time • Widely available	• Limited for volumetric or 3D analysis • May miss small cartilage defects	• Detection of cartilage surface irregularities, fissures, and thinning • Early osteoarthritis assessment • Traumatic chondral injuries • Synovitis or bone marrow edema
3D gradient echo (SPGR, DESS, and FLASH)	3D isotropic gradient echo techniques	• High spatial resolution • Enables multiplanar reformatting—allows volumetric and quantitative analysis • Ideal for cartilage morphology assessment	• Lower SNR than spin echo • More sensitive to susceptibility artifacts • Subchondral bone marrow edema is not well depicted	• Measuring cartilage thickness and volume • Detecting focal defects • Monitoring disease progression or therapy response • Preoperative planning for cartilage repair
3D FSE (SPACE, CUBE, and VISTA)	3D spin echo with isotropic resolution	• Combines 3D acquisition with spin echo contrast • High SNR • Less affected by magnetic field inhomogeneities • Suitable for metallic implants	• Longer acquisition time compared to GRE • Requires advanced postprocessing	• Comprehensive joint evaluation (cartilage, menisci, ligaments, and subchondral bone) • Osteoarthritis research—Imaging near metallic implants
Balanced steady-state free precession	Rapid gradient echo with balanced gradients	• Very fast acquisition • High signal from cartilage and joint fluid • Excellent contrast • Good for motion prone patients	• Sensitive to field inhomogeneities • Less suitable for detailed structural evaluation	• Screening joint integrity • Pediatric imaging • Quick assessment of cartilage thickness and surface continuity

Abbreviations: CUBE, 3D fast spin-echo sequence (CUBE)GE para una secuencia 3D FSE (*Cube* suele dejarse como nombre propio; puede; DESS, double-echo steady-state; FLASH, fast low-angle shot; GRE, gradient-recalled echo; VISTA, volume isotropic turbo spin echo acquisition.

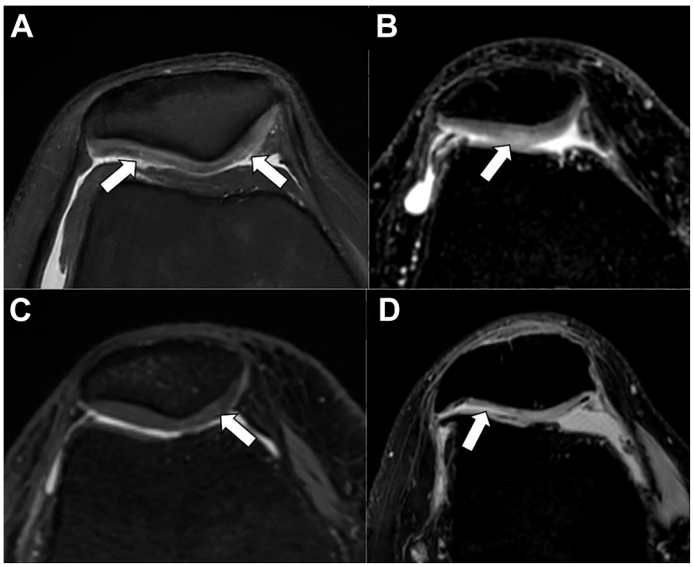

Fig. 3. Summary of main morphologic MR imaging sequences. (*A*) Axial 2D PD FSE fat-saturated image reveals superficial fissures, affecting less than 50% of the cartilage thickness in the patellar facets, a grade II lesion on the Outerbridge classification, and 2 A Noyes (*arrows*). (*B*) Axial 3D T2 Space fat-suppressed image reveals focal high signal in the lateral patellar facet, compatible with edema, a grade I lesion on the Outerbridge and Noyes modified classification (*arrow*). (*C*) Axial 3D True FIST with fat saturated image reveals a focal high signal in the medial patellar facet, compatible with edema, without clear fissures, indicating a grade I lesion (*arrow*). (*D*) Axial 3D SPGR with fat-saturated image showing femoro patellar joint space narrowing with diffuse chondral loss, more prominent on the lateral facet, without subchondral bone edema, a degenerative grade II lesion (*arrow*).

Table 2
Summary of functional MR imaging sequences for cartilage assessment

Technique	Main Target/Principle	Clinical Use	Advantages	Limitations
T2 mapping	Measures interaction of water with collagen fibers (T2 relaxation)	Early OA detection, collagen integrity, and postrepair evaluation	No contrast needed, available at 1.5–3T, detects early matrix damage	Affected by magic angle effect, limited in deep layers, nonspecific for PG loss
T1rho mapping	Spin-lattice relaxation in rotating frame; sensitive to proteoglycan content	Detects early OA and PG loss; complements T2 mapping	Sensitive to early ECM changes, no contrast required	Long acquisition and postprocessing; requires specific RF pulse
dGEMRIC	Uses Gd-DTPA^{2-} contrast inversely related to GAG concentration (T1 shortening)	Quantifies GAG loss in OA, hip dysplasia, and therapy monitoring	Quantitative biochemical assessment; well-validated	Requires double dose of gadolinium, long delay (>60 min), complex protocol
DWI/DTI	Analyzes diffusion of water molecules; MD and FA reflect ECM structure	Evaluates cartilage microstructure, early OA, collagen, and PG organization	Noninvasive, sensitive to microstructural changes	Technically demanding; low SNR, motion and susceptibility artifacts
gagCEST	Measures proton exchange between GAG-bound and free water pools	Detects GAG depletion, monitors repair and early OA	No contrast agent, specific for GAGs	Requires high field ($\geq$3T), sensitive to B0 inhomogeneity, long scan time
Sodium MR imaging	Detects ^{23}Na ions bound to negatively charged PGs; reflects fixed charge density	Quantifies GAG concentration, evaluates OA progression	Direct assessment of PG content; specific biochemical marker	Low SNR, short T2*, long scans, and limited clinical availability

Abbreviations: ECM, extracellular matrix; MD, mean diffusivity; OA, osteoarthritis; PG, proteoglycan(s).

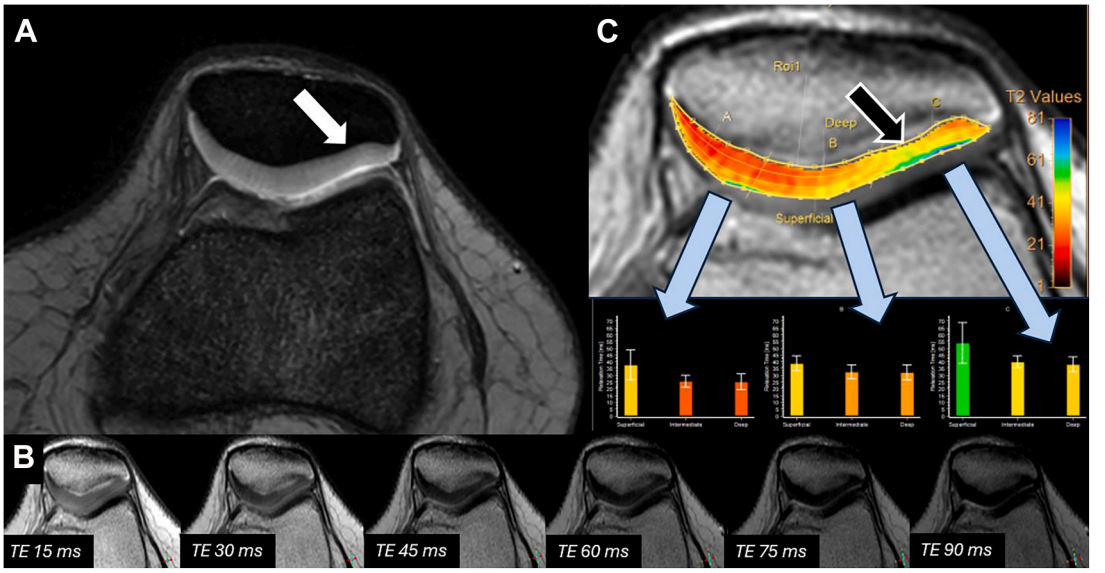

Fig. 4. (*A–C*) A 29 year old male patient with knee pain. (*A*) Conventional fast field echo acquisition (FFA) image demonstrates subtle increased signal intensity at the lateral patellar facet (*white arrow*). (*B*) Multiecho T2 mapping imatge acquisition (*C*) Color-coded T2 map shows a larger area of elevated superficial T2 values at the corresponding location (*black arrow*), consistent with early chondromalacia. Blue arrows indicate regions of interest used for quantitative T2 analysis and their corresponding T2 value plots.

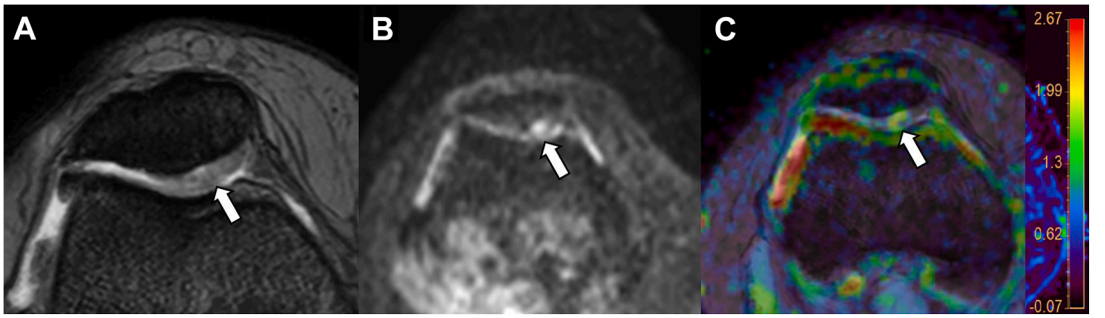

Fig. 5. DWI assessment of hyaline cartilage. A 56 year old female patient with knee locking. (*A*) Conventional T2 FFE shows degenerative changes and focal hyperintensity (*arrow*); (*B*) DWI (b = 800 s/mm^2) confirms signal increase (*arrow*); (*C*) Fusion with ADC map shows correlated elevation suggesting collagen matrix los (*arrow*).

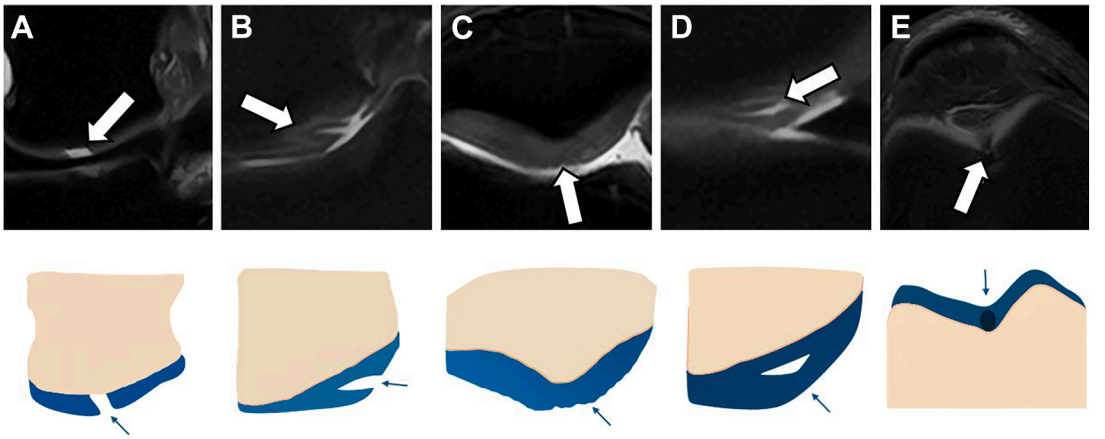

Fig. 6. Proton density fat-saturated images and schematic descriptors: (*A*) Defect—localized height los (*arrow*); (*B*) Delamination—cartilage layer separation without subchondral bone detachment (*arrow*); (*C*) Fibrillation—superficial fissure less than 1 mm (*arrow*); (*D*) Deep fissure—basal delamination visible only on MR imaging (*arrow*); (*E*) Dark cartilage—low signal due to degeneration or calcinosis (*arrow*).

Table 3
Glossary of terms related to cartilage damage

Term	Description
Defect	Used as a synonym for ulceration or erosion, and should be used when there is a localized loss of height, sharply marginated and well shouldered. It is relevant to report the size and localization. In the knee, a small defect is around 2–9 mm, moderate size 10–19 mm, and large defect 20–29 mm
Degeneration, chondrosis, or softening	Synonyms for chronic appearance lesions
Delamination	Refers extension of the fissure parallel to the surface of the bone. It is advisable to measure its extension and determine whether there is an associated flap
Fibrillation	Superficial fissuring of <1 mm
Deep chondral fissures	Lesions that do not extend to the surface may result in basilar delamination (the deep cartilage layer separates from the subchondral bone) detectable by MR imaging but not visible with arthroscopy
Chondral lesion	General term used when the subchondral bone is intact
Osteochondral lesion (OCL)	Used when both articular cartilage and underlying bone are compromised. This term is not specific and a more detailed description is preferred. Specific staging systems such as the Hepple classification or the OCL grading system by the ICRS adapted for MR imaging are recommended to establish lesion stability
Osteochondritis dissecans	Used when an injury appears in developing subchondral bone. It has an independent surgical staging system consisting of IV stages based on fragment stability
Dark cartilage lesions	Can represent low signal intensity chondral degeneration or chondrocalcinosis that may progress to cartilage loss and is associated with cartilage fissuring on arthroscopy

Data from Fritz RC, Chaudhari AS, Boutin RD. Preoperative MRI of Articular Cartilage in the Knee: A Practical Approach. J Knee Surg 2020;33(11):1088–1099. https://doi.org/10.1055/s-0040-1716719.

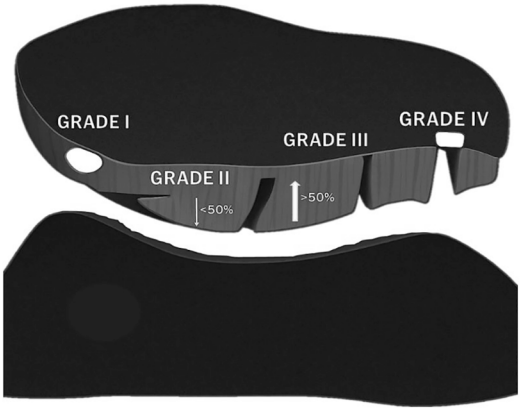

Fig. 7. Classification of structural cartilage damage by signal and depth: Grade 0—normal; Grade 1—edema/minor fissures; Grade 2—partial defect less than 50%; Grade 3—partial defect greater than 50%; Grade 4—full-thickness loss ± subchondral bone involvement.

defects exceeding 50%, full thickness cartilage loss with and without subchondral bone involvement (**Fig. 7**).

Classification Systems

Modified Outerbridge classification

The modified Outerbridge classification divides chondral lesions into 5 grades (0–IV) based on depth and surface involvement.[17] It is simple and reproducible for moderate and severe defects, but mild (Grade I) lesions may be difficult to detect on MR imaging because of subtle signal alterations (**Box 1**, **Fig. 8**).

International Cartilage Repair Society classification

The ICRS grading system[18] provides greater detail and interobserver reliability (κ up to 0.8), describing lesion depth and subchondral involvement with arthroscopic and MR imaging correlation. The grades range from 0 to 4 (**Box 2**, **Fig. 9**).

Box 1
Modified Outerbridge classification

Grade	Description	Figure
GRADE 0	Normal cartilage. No MR imaging alterations	Fig. 2
GRADE I	Edema with intact surface. Increased cartilage signal on MR imaging	Fig. 8A, B
GRADE II	Partial-thickness superficial defect, affecting <50% of the cartilage. Includes fissures and fragmentation. Typically, small (<1.5 cm)	Fig. 8C
GRADE III	Partial-thickness defect exceeding 50% or full-thickness cartilage loss without subchondral bone involvement. Larger areas (>1.5 cm)	Fig. 8D
GRADE IV	Full-thickness cartilage loss with subchondral bone involvement	Fig. 8E, F

Noyes and stable's grading system

The Noyes–Stabler system[19] integrates lesion localization, particularly in the patellofemoral compartment, improving communication with surgeons but increasing complexity (**Box 3**).

MR imaging scales for cartilage evaluation

Semiquantitative whole-joint MR imaging scores, such as WORMS (Whole-Organ MRI Score), MOAKS (MRI Osteoarthritis knee score), WOAKS (Whole-Organ Arthroscopic Knee Score), BLOCKS (Boston-Leeds Osteoarthritis Knee Score), and AMADEUS (Area Measurement And Depth and Underlying Structures Score) are more thorough,[20–22] but they are more complex so they are usually limited for research.[23]

IMAGE-GUIDED THERAPY

Image-guided intra-articular therapies are pivotal in minimally invasive management. Ultrasound guidance is most common, offering real-time visualization and safety in superficial joints.[24] MR imaging and MR imaging–US fusion enhance precision for regenerative procedures. Therapeutic options include hyaluronic acid (HA) for lubrication, corticosteroids for inflammation control, and platelet-rich plasma (PRP) for anti-inflammatory and

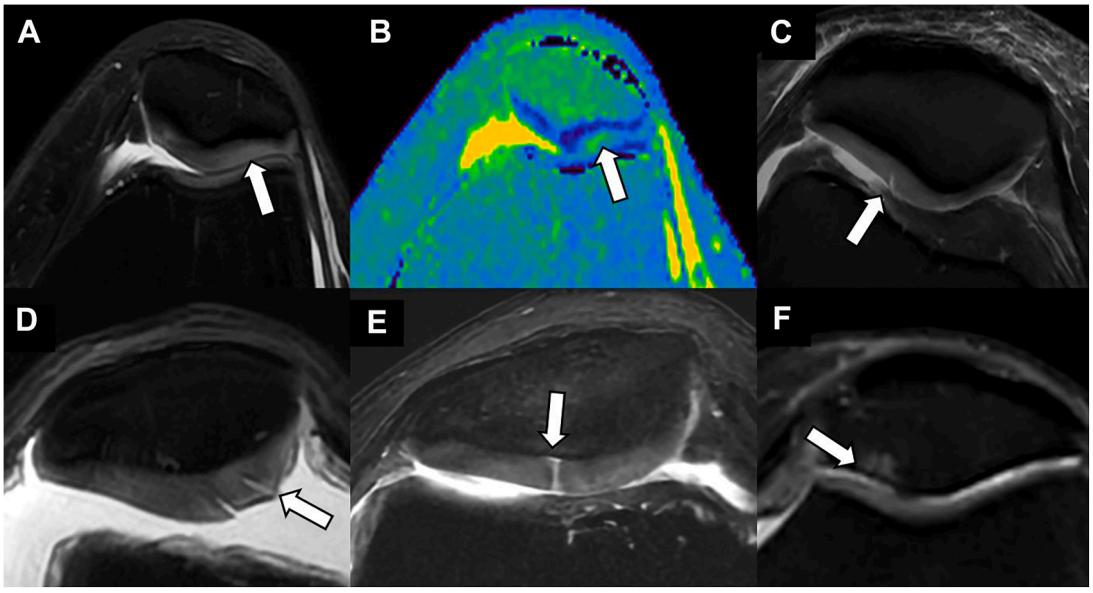

Fig. 8. Outerbridge grades of chondromalacia. (*A*) A fat-suppressed T2-weighted axial image reveals focal high signal (*arrow*) and (*B*) T2 relaxation time is increased on T2 mapping (*arrow*), compatible with edema in the lateral patellar facet, a grade I lesion. (*C*) A fat-suppressed T2-weighted axial image shows a superficial partial thickness high signal intensity chondral fissure, affecting less than 50% of the cartilage thickness (*arrow*), a grade II lesion and (*D*) affecting more than 50% of the patella cartilage thickness (*arrow*), a grade III lesion. (*E*) A fat-suppressed T2-weighted axial image shows a full thickness fissure without bone involvement (*arrow*) and (*F*) diffuse chondral loss with subchondral bone edema (*arrow*).

Box 2
International Cartilage Repair Society classification

Grade	Description	Subdivision
ICRS grade 0	Normal cartilage. No lesions are present	
ICRS grade 1	Superficial mild lesions	(1a) Signal abnormalities on an intact surface (1b) Fibrillations and fissures limited to the external layers
ICRS grade 2	Partial-thickness defect affecting <50% of cartilage. It can be an ulcer, a fissure or cartilage loss that does not affect deep layers	
ICRS grade 3	Partial-thickness defect exceeding 50% without subchondral bone exposure. Delamination and chondral flaps are included	
ICRS grade 4	Severely abnormal Full-thickness lesions with complete cartilage loss and bone exposure	(4a) Subchondral plate involvement (4b) Osteochondral deep lesion (eg, cystic formations)

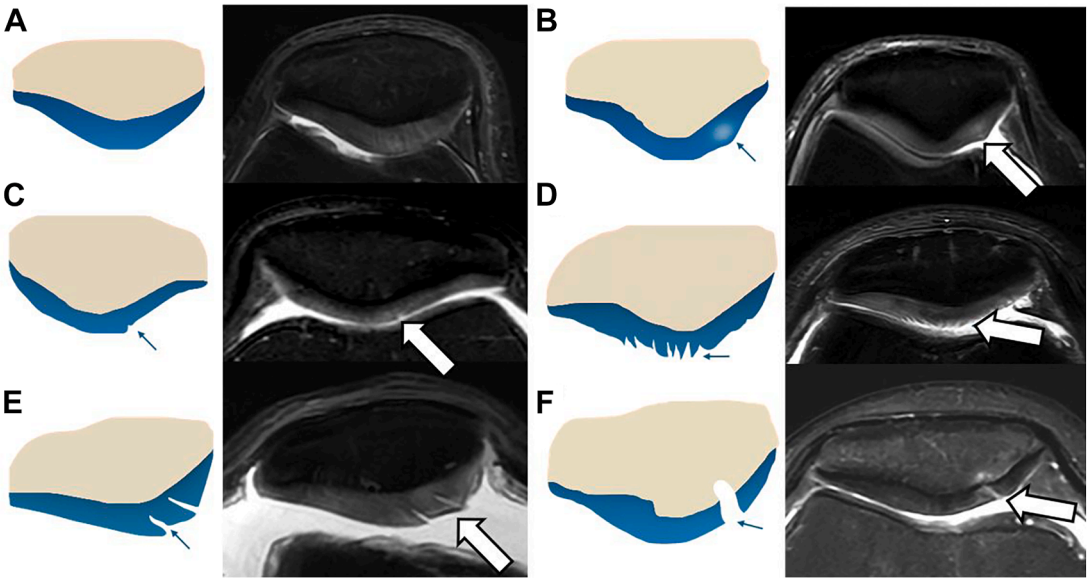

Fig. 9. ICRS grading system. (*A*) Normal; (*B*, *C*) Grade 1—surface signal or mild fibrillation (*arrows*); (*D*) Grade 2—defect less than 50% (*arrows*); (*E*) Grade 3—defect greater than 50% (*arrows*); (*F*) Grade 4—full-thickness loss with subchondral or osteochondral involvement (*arrows*).

Box 3
Noyes and Stable's gradings system

Grade	Description	Subdivision
GRADE 0	Normal cartilage, no MR imaging findings	
GRADE 1	Cartilage surface intact with high T2 signal	
GRADE 2	Damaged cartilage surface	2A: Superficial partial-thickness defects affecting <50% of the cartilage 2B: Deep partial-thickness defects exceeding 50% of cartilage thickness
GRADE 3	Full-thickness lesion with bone surface exposition	3A: Without subchondral lesions 3B: With subchondral lesions such as bone edema and osteophyte

Table 4
Magnetic resonance observation of cartilage repair tissue 2.0 classification for repaired cartilage

Parameter	Description/Categories	Score
Degree of defect repair and filling of defect	Complete filling of defect	20
	Hypertrophy of repair tissue	15
	Incomplete filling (≥50% of adjacent cartilage)	10
	Incomplete filling (<50% of adjacent cartilage)	5
	Subchondral bone exposed	0
Integration to border zone	Complete integration with adjacent cartilage	15
	Demarcating border visible (without defect)	10
	Defect <50% of length of repair tissue at border	5
	Defect >50% of length of repair tissue at border	0
Surface of repair tissue	Surface intact and smooth	10
	Surface damaged (<50% of repair area)	5
	Surface damaged (>50% of repair area)	0
Structure of repair tissue	Homogeneous structure	10
	Inhomogeneous structure	0
Signal intensity of repair tissue (T2 or PD images)	Identical to native cartilage	15
	Nearly identical (minor differences)	10
	Moderately different	5
	Markedly different	0
Subchondral lamina	Intact	5
	Not intact	0
Subchondral bone	Intact	5
	Edema/granulation tissue/cysts/sclerosis	0
Adhesions	No adhesions	5
	Presence of adhesions	0
Effusion	No effusion	5
	Effusion	0

Maximum total score: 100 points.
100 = Normal (excellent repair). 70–99 = Good repair. 40–69 = Moderate repair. Less than 40 = Poor repair.

Table 5
Summary of MR imaging evolution findings by technique

Technique	Summary of MR Imaging Evolution
Microfracture (MFX)	Early fibrocartilage is thin and T_2-hyperintense with subchondral edema. Persistent edema >18 mo suggests poor maturation
ACI/MACI	Initially high T_2 signal normalizes by 12–24 mo; persistent edema or thickened interface indicates possible graft failure
OAT/Mosaicplasty	Bone marrow edema resolves by 6–9 mo; persistence beyond 18 mo indicates incomplete integration
OCA	Similar to OAT; focus on junctional integration and uniform graft signal; artifacts may interfere
Cellular/Scaffold-based repair	Early homogeneous T_2-hyperintense tissue matures gradually; MR imaging monitors scaffold resorption; long-term data limited
PRP	Decreased T_2 at 12 mo correlates with biochemical improvement; no morphologic change
HA	Temporary T2 reduction and clinical relief at 3 mo, returning to baseline by 9–15 mo; less durable effect than PRP

Abbreviations: ACI/MACI, autologous chondrocyte implantation; Cellular or Scaffold-Based Matrix Repair (eg, MSC or collagen scaffolds); HA, intra-articular hyaluronic acid; MFX, microfracture; OAT/Mosaicplasty, osteochondral autograft transfer; OCA, osteochondral allograft; PRP, intra-articular platelet-rich plasma.

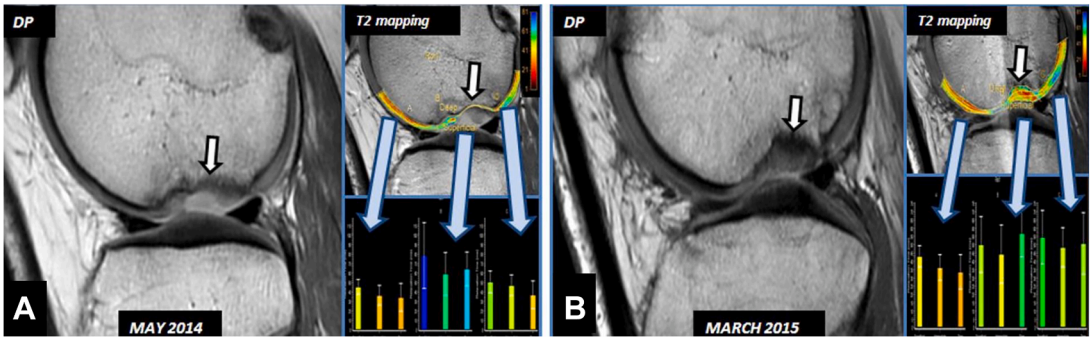

Fig. 10. Matrix chondrocyte transplantation monitoring. (*A*) A 35 year old male patient with chondral lesion at external condyle (*arrows*) that shows a practically complete loss of cartilage surface with severe increase of T2 values at central condyle area, underwent cartilage repair surgery (matrix-associated chondrocyte transplantation). (*B*) A new MR imaging study with T2 mapping was performed 10 months later that showed recovery of condylar cartilage cover (*arrows*) with normalization of T2 values with regard to rest of hyaline cartilage.

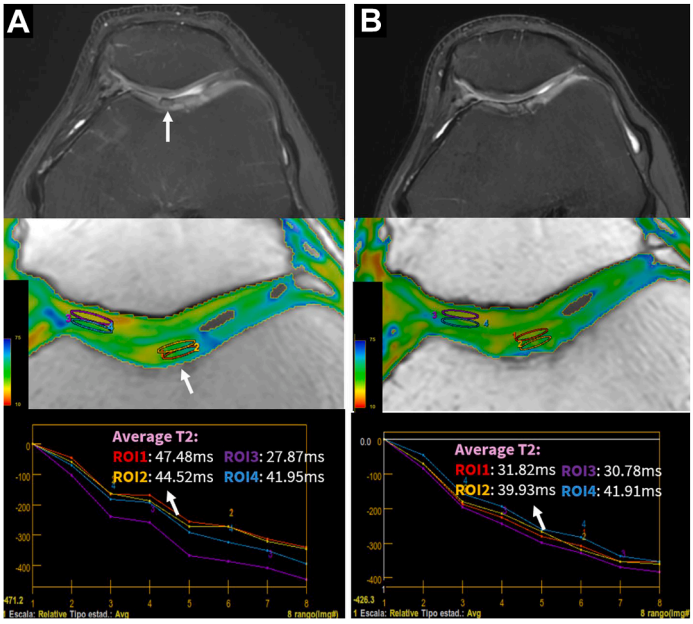

Fig. 11. Autologous chondrocyte implantation monitoring. A 48 year old male patient with chondral delamination of the central trochlea (*arrow*) underwent autologous chondrocyte implantation Instant Cemtro Cell (ICC) repair.[35] (*A*) A 12 month follow-up T2map demonstrates elevated water content (*arrow*) at both deep and superficial layers compared to control adjacent patellar region. (*B*) A 24 month follow-up T2map shows lower water content (*arrow*) consistent with a greater fibrous tissue component in the repair zone. (*Courtesy of* Eugenia Sánchez, Clínica Cemtro, Madrid, Spain; and Laura Carretero, GE HealthCare; and Guillén-García P, Guillén-Vicente I, Rodríguez-Iñigo E, et al. Cartilage Defect Treatment Using High-Density Autologous Chondrocyte Implantation (HD-ACI). Bioengineering. 2023;10(9):1083. https://doi.org/10.3390/bioengineering10091083.)

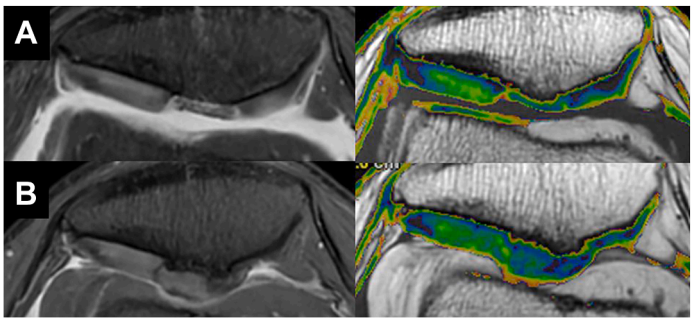

Fig. 12. Follow-up after bone marrow aspirate concentrate (BMAC) based graft treatment. A 35 year old female patient with a Grade 4 ICRS (International Cartilage Repair Society) patellar chondral defect. Repair technique used a Chondro-Gide + BMAC bioscaffold-based graft. Axial T2 fat-saturated with corresponding T2 mapping MR images acquired at 6 (*A*) and 29 (*B*) months postsurgery. Initially thin at the 6 months, the graft demonstrates improved thickness and maturation by the 29 month, showing a homogeneous signal and T2 Relaxation Time color distribution pattern, indicating a mature, well-integrated, and durable cartilage repair with no separation from the adjacent native articular cartilage. (*Courtesy of* Steven Wong, Sengkang General Hospital, Singapore.)

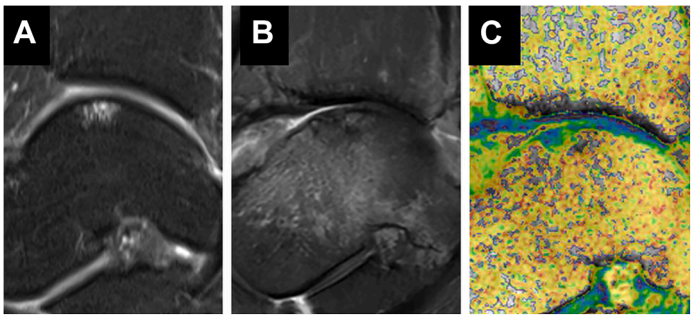

Fig. 13. A 67 year old patient follow-up after a BMAC bioscaffold-based graft anchored for a talar dome defect. (*A*) Sagittal T2 fat-saturated image shows a partial-thickness defect in the talar dome. (*B*) Sagittal T2 fat-saturated image with T2 mapping (*C*) after 11 months postoperative demonstrates the repair graft filling the talar dome defect. T2 mapping allows superior visualization and quantitative assessment of the repair tissue, revealing a low-to-mid T2 relaxation value range and a homogeneous color distribution throughout the graft. This pattern is consistent with mature, fibrocartilaginous repair tissue and stable integration with the surrounding cartilage. (*Courtesy of* Steven Wong, Sengkang General Hospital, Singapore.)

regenerative stimulation. Mesenchymal stem cells (MSCs) support chondrogenesis through paracrine and differentiation mechanisms, though most applications remain investigational.[25] Scaffold-based and 3D-printed biotherapies integrating MSCs or PRP are emerging as next-generation options.[26]

POSTTREATMENT IMAGING

MR imaging is the preferred modality for postoperative follow-up after cartilage repair, allowing noninvasive assessment of graft maturation, integration, and subchondral bone status. Morphologic sequences evaluate surface regularity and defect filling, while quantitative mapping techniques such as T2 and T1rho mapping provide insight into collagen integrity and proteoglycan content.[27] The Magnetic Resonance Observation of Cartilage Repair Tissue (MOCART) scoring system, updated to MOCART 2.0 in 2021,[28] standardizes evaluation with objective criteria across nine parameters (**Table 4**), improving reproducibility for clinical trials and follow-up studies.

Postoperative MR imaging findings depend on the repair technique.[29] **Table 5** provides a summary of the MR imaging findings for different techniques. Microfracture typically forms fibrocartilage with initial high T2 signal that gradually normalizes as the tissue matures.[30] Osteochondral autograft transfer (OAT) usually restores surface continuity within 12 to 18 months; persistent edema or fissuring indicates poor osseous integration. Osteochondral allograft transplantation (OCA) should be monitored for marrow edema and interface irregularities, which suggest graft failure.[31] Autologous chondrocyte implantation (ACI), or matrix-ACI demonstrates early hyperintensity and progressive zonal organization toward native cartilage architecture (**Figs. 10** and **11**). Complications such as cysts, hypertrophy, or delamination may occur. Subchondral cysts larger than approximately 5 to 10 mm, especially if progressive or associated with edema, should be considered a negative prognostic sign after cartilage repair—but size alone is insufficient to define failure.[32] Biological therapies such as PRP, HA, and MSCs show variable MR imaging responses,[33] reflecting the evolving regenerative mechanisms rather than structural graft formation.[34] Combined hybrid techniques using biological and scaffold-based graft procedures are currently used. Morphologic MR imaging sequences combined with T2 mapping images provide an optimal analysis for follow-up outcome (**Figs. 12** and **13**).[3]

SUMMARY

MR imaging plays a central role in the modern evaluation and management of cartilage injury. The integration of high-resolution morphologic imaging, advanced quantitative mapping, and image-guided regenerative techniques has revolutionized diagnosis, monitoring, and therapy. Emerging technologies such as AI-assisted reconstruction, compositional MR imaging, and hybrid interventions promise earlier detection and personalized treatment of cartilage degeneration, improving outcomes and long-term joint preservation.

CLINICS CARE POINTS

- MR imaging—particularly high-resolution morphologic and advanced functional techniques—enables early detection of cartilage degeneration and objective monitoring of repair and therapeutic response, guiding personalized treatment.
- Ultrasound and MR imaging-guided intra-articular injections improve precision and safety in delivering regenerative and anti-inflammatory treatments-based therapies.

DISCLOSURE

The authors declare that they have no conflicts of interest to disclose related to this study.

REFERENCES

1. Hunter DJ, Bierma-Zeinstra S. Osteoarthritis. Lancet 2019;393(10182):1745–59.
2. Fernandes TL, SantAnna JPC, Fiorio BA, et al. State of the art for articular cartilage morphological and composition imaging evaluation in football players. J Cartil Jt Preserv 2022;2(2). https://doi.org/10.1016/j.jcjp.2022.100067.
3. Chalian M, Li X, Guermazi A, et al. The QIBA profile for MRI-based compositional imaging of knee cartilage. Radiology 2021;301(2):423–32.
4. Sophia Fox A, Bedi A, Rodeo S. The basic science of articular cartilage: structure, composition, and function. Sports Health 2009;1(6):461–8.
5. Kijowski R. 3D MRI of articular cartilage. Semin Musculoskel Radiol 2021;25(3):397–408.
6. Buchanan ME, Markhardt BK. Systematic review of techniques in cartilage imaging. J Cartil Jt Preserv 2024;4(1):100155.
7. Willaume T, Ehlinger M, Favreau H, et al. Assessment of knee cartilage using accelerated 3 T MRI: evaluation of an isotropic 3D fast spin-echo sequence (CUBE) with compressed sensing technique. Magn Reson Imaging 2025;117:110321.
8. Shah AJ, Patel D. Imaging update on cartilage. J Clin Orthop Trauma 2021;22:101610.
9. Cheng KY, Moazamian D, Ma Y, et al. Clinical application of ultrashort echo time (UTE) and zero echo time (ZTE) magnetic resonance (MR) imaging in the evaluation of osteoarthritis. Skelet Radiol 2023;52(11):2149–57.
10. Martín Noguerol T, Raya JG, Wessell DE, et al. Functional MRI for evaluation of hyaline cartilage extracellular matrix, a physiopathological-based approach. Br J Radiol 2019;92(1103):20190443. https://doi.org/10.1259/bjr.20190443.
11. Mosher TJ. Quantitative cartilage T2 and T1rho mapping: is there a clinical role? From the AJR special series on quantitative imaging. Am J Roentgenol 2025;224(5):e2431655. https://doi.org/10.2214/AJR.24.31655.
12. Lee JH, Houck DA, Gruizinga BA, et al. Correlation of delayed gadolinium-enhanced MRI of cartilage (dGEMRIC) value with hip arthroscopy intraoperative findings and midterm periacetabular osteotomy outcomes. Orthop J Sports Med 2022;10(9):23259671221117606. https://doi.org/10.1177/23259671221117606.
13. Raya J e G, Duarte A, Wang N, et al. Applications of diffusion-weighted MRI to the musculoskeletal system. J Magn Reson Imaging 2024;59(2):376–96.
14. Soellner ST, Welsch GH, Gelse K, et al. gagCEST imaging at 3 T MRI in patients with articular cartilage lesions of the knee and intraoperative validation. Osteoarthr Cartil 2021;29(8):1163–72.
15. Fritz RC, Chaudhari AS, Boutin RD. Preoperative MRI of articular cartilage in the knee: a practical approach. J Knee Surg 2020;33(11):1088–99.
16. Markhardt BK, Huang BK, Spiker AM, et al. Interpretation of cartilage damage at routine clinical MRI: how to match arthroscopic findings. Radiographics 2022;42(5):1457–73.
17. Slattery C, Kweon CY. Classifications in brief: outerbridge classification of chondral lesions. Clin Orthop 2018;476(10):2101–4.
18. Dwyer T, Martin CR, Kendra R, et al. Reliability and validity of the arthroscopic international cartilage repair society classification system: correlation with histological assessment of depth. Arthrosc J Arthrosc Relat Surg 2017;33(6):1219–24.
19. Noyes FR, Stabler CL. A system for grading articular cartilage lesions at arthroscopy. Am J Sports Med 1989;17(4):505–13.
20. Alizai H, Virayavanich W, Joseph GB, et al. Cartilage lesion score: comparison of a quantitative assessment score with established semiquantitative MR scoring systems. Radiology 2014;271(2):479–87.
21. Heinz T, Meller F, Luetkens KS, et al. Can the MRI based AMADEUS score accurately assess presurgery chondral defect severity according to the ICRS arthroscopic classification system? J Exp Orthop 2022;9(1):83.
22. Spahn G, Muckley T, Klinger HM, et al. Whole-organ arthroscopic knee score (WOAKS). BMC Musculoskelet Disord 2008;9(1):155.
23. Grace T, Neumann J, Samaan MA, et al. Using the scoring hip osteoarthritis with magnetic resonance imaging (SHOMRI) system to assess intra-articular pathology in femoroacetabular impingement. J Orthop Res 2018;36(11):3064–70.
24. Sibbitt W, Peisajovich A, Michael AA, et al. Does ultrasound guidance improve the outcomes of arthrocentesis and corticosteroid injection of the knee? J Rheumatol 2009;36(9):1892–902.
25. Barry F, Murphy M. Mesenchymal stem cells in joint disease and repair. Nat Rev Rheumatol 2013;9(10):584–94.
26. Di Bella C. 3D bioprinting of cartilage for orthopedic applications: current status and future perspectives. J Orthop Res 2018;36(1):23–32.
27. Stewart ZE, Joseph Simeone F, Guermazi A, et al. Postoperative imaging of cartilage: where are we in 2023? J Cartil Jt Preserv 2024;4(1):100150.
28. Schreiner MM, Raudner M, Röhrich S, et al. Reliability of the MOCART (Magnetic Resonance Observation of Cartilage Repair Tissue) 2.0 knee score for different cartilage repair techniques—a retrospective observational study. Eur Radiol 2021;31(8):5734–45.

29. Zheng Y, Wong SBS, Peter CA, et al. Evaluation of the patella following cartilage repair on conventional magnetic resonance imaging and T2 mapping. Clin Radiol 2025;88:107006.
30. Polster J, Recht M. Postoperative MR evaluation of chondral repair in the knee. Eur J Radiol 2005; 54(2):206–13.
31. Cobianchi Bellisari F, De Marino L, Arrigoni F, et al. T2-mapping MRI evaluation of patellofemoral cartilage in patients submitted to intra-articular platelet-rich plasma (PRP) injections. Radiol Med (Torino) 2021;126(8):1085–94.
32. Gao L, Cucchiarini M, Madry H. Cyst formation in the subchondral bone following cartilage repair. Clin Transl Med 2020;10(8):e248.
33. Ho KK-W, Lee WY-W, Griffith JF, et al. Randomized control trial of mesenchymal stem cells versus hyaluronic acid in patients with knee osteoarthritis – a Hong Kong pilot study. J Orthop Transl 2022;37: 69–77.
34. Vogrin M, Naranda J, Gorenjak M, et al. T2 mapping evaluation of changes in cartilage matrix after PRP and HA injection therapy in knee osteoarthritis: a prospective, randomized, double blind, placebo controlled study. In: In review. 2020. https://doi.org/10.21203/rs.3.rs-36493/v1.
35. Guillén-García P, Guillén-Vicente I, Rodríguez-Iñigo E, et al. Cartilage defect treatment using high-density autologous chondrocyte implantation (HD-ACI). Bioengineering 2023;10(9):1083.